JOURNAL OF MATERIALS SCIENCE 31 (1996) 3567–3572

Silicide formation by solid-state diffusion in MO/Si multilayer thin films

EUNGJOON CHI, JAEYEOB SHIM, JOONSEOP KWAK, HONGKOO BAIK
Department of Metallurgical Engineering, Yonsei University, Seoul 120-749, Korea

The solid-state reaction of Mo/Si multilayer thin films produced by the r.f. magnetron sputtering technique was examined using differential scanning calorimetry (DSC) and X-ray diffraction and was explained by the concepts of effective driving force and effective heat of formation. In constant scanning-rate DSC, there were two exothermic peaks representing the formation of h-$MoSi_2$ and t-$MoSi_2$, respectively. The activation energy for the formation of h-$MoSi_2$ was 1.5 eV, and that of t-$MoSi_2$ was 7.8 eV. Nucleation was the rate-controlling mechanism for each silicide formation. The amorphous phase was not formed in the Mo/Si system as predicted by the concept of effective driving force. h-$MoSi_2$, the first crystalline phase, was considered to have lower interfacial free energy than t-$MoSi_2$, and by increasing the temperature, it was transformed into more stable t-$MoSi_2$.

1. Introduction

Polycrystalline silicon used as gate electrode and interconnecting material shows limitation due to high resistance and high-temperature instability. As a substitutional material, refractory metal silicide has caught attention [1]. This silicide is formed through deposition and heat treatment. During these procedures, amorphous and crystalline phases are formed through solid-state diffusion. Amorphous phase is the first phase formed at the time of deposition in thin films and affects the formation of crystalline phase. A crystalline phase starts to form when amorphous phase reaches a critical thickness [2]. In the case of thin film, all the crystalline phases existing in equilibrium phase diagram do not form simultaneously, nor does the most stable crystalline phase form at once, but the final phase is reached through sequential steps [3]. Therefore, a study of the formation and growth of amorphous and crystalline phase stages is necessary to control the reliability and the electrical property of a semiconductor device.

It is well known that the amorphous phase formation by solid-state reaction is due to the fast diffusion of one element. If the fast atom diffuses to the matrix and increases beyond the critical concentration, an amorphous layer is formed as the stress induced within the matrix disturbs the matrix structure [4]. Because the regular arrangement of the matrix is disturbed by the fast-diffusing atom, a thermodynamically stable crystalline phase cannot be formed. Therefore, it is essential to study the relation of the thermodynamical driving force and the kinetic factors to the formation of amorphous and crystalline phase by solid-state diffusion.

In this study, the solid-state reaction of Mo/Si multilayer thin film was investigated. The Mo/Si multilayer thin film can be used mainly in two technological fields. First, the Mo/Si multilayer thin film itself is used as an X-ray monochromator [5]. The monochromator is made up of a multilayer structure of heavy metal and silicon (or carbon). Among these, the Mo/Si system is the most efficient monochromator in the soft X-ray region having a wavelength of 13–30 nm due to high reflectance. This optical quality is very sensitive to mutual diffusion and compound formation at the thin film interface. Thus thermal and chemical stability of the interface is greatly required. Second, Mo-silicide is used as an interconnecting material for semiconductor devices like other silicides, because of high-temperature stability and low resistivity. Because the interface reaction can affect the property of the silicide formed, successfully to produce a semiconductor device, it is necessary to understand phase transition and the formation mechanism.

Solid-state reaction of the Mo/Si multilayer thin film was examined using differential scanning calorimetry (DSC) and X-ray diffraction (XRD). DSC analysis has the following advantages. First, it is more sensitive to composition and structure change compared to other methods. Second, both thermodynamic and kinetic information on the phase transition can be obtained through a single experiment. The exact temperature and activation energy of each reaction were acquired through constant scanning-rate DSC analysis, and the mechanism of phase formation through isothermal DSC analysis.

Many theoretical models have been proposed in order to predict the formation of amorphous phase and the phase sequence of crystalline phase in a thin film. In this study, the concept of effective driving force proposed, by Kwak *et al.* [6], was applied to predict the formation of an amorphous phase. In addition, the

0022–2461

effective heat of formation proposed by Pretorius *et al.* [7] has been used to explain the phase transition of crystalline phases.

2. Experimental procedure

Mo/Si multilayer thin films were deposited by an r.f. magnetron sputtering apparatus. The vacuum level of the chamber was set below 1.0×10^{-6} torr (1 torr = 133.322 Pa) before deposition, and during the deposition it was maintained at 5.0×10^{-3} torr. The purity of the molybdenum and silicon targets, 4 in in diameter, was 99.95% and 99.999%, respectively. To prepare free-standing film, NaCl was used as the substrate. To enlarge the interface area per unit volume of thin films, ten each of molybdenum and silicon layers were alternately deposited. In order to prevent oxidation of molybdenum, the top and bottom layers were of silicon. The atomic concentration ratio of molybdenum and silicon was set at 1–2. The thickness of one bilayer was 75 nm, which brings the total thickness of the specimen to 750 nm. The amount of specimen used per DSC analysis was about 1–2 mg. In order to determine the activation energy of phases formed by solid-state reactions, the heating rate was varied by 20, 10, 5 and 2.5 °C min^{-1} during the constant scanning-rate DSC. For the isothermal DSC, films were heated at 200 °C min^{-1} to a desired temperature and maintained for 2 h at that temperature. After the DSC analysis, X-ray diffraction technique was used to examine the crystalline phases formed.

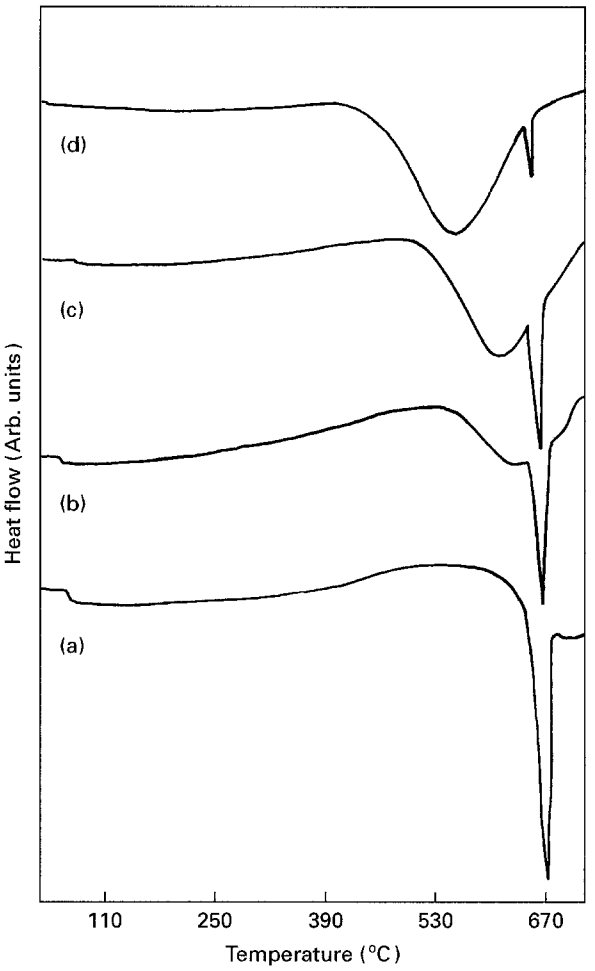

Figure 1 Constant scanning-rate DSC traces for Mo/Si multilayer thin films heated at (a) 20, (b) 10, (c) 5 and (d) 2.5 °C min^{-1}.

3. Results and discussion

3.1. Phase transition and reaction mechanism

To check the first crystalline phase, phase transition and amorphization by solid-state reaction, the film was heated from 30 °C to 700 °C at 20, 10, 5 and 2.5 °C min^{-1} and the DSC curve traces are shown in Fig. 1. In Fig. 1, two exothermic peaks appeared. These peaks moved down to a lower temperature as the heating rate slowed down. In order to identify the reaction in the first peak, a sample was heated to 630 °C which is the temperature immediately before the second peak starts. The results of XRD analysis of this sample and the as-deposited sample are shown in Fig. 2. Only peaks relating to unreacted molybdenum and hexagonal $MoSi_2$ (h-$MoSi_2$) appear in Fig. 2b, which indicates that the first exothermic peak represents the formation of h-$MoSi_2$.

Fig. 3 shows the XRD patterns of the specimens heated to 700 °C at various heating rates. With some h-$MoSi_2$ still existing in Fig. 3c and d, tetragonal $MoSi_2$ (t-$MoSi_2$) peaks appeared independently of the heating rate. Thus, it is confirmed that the second exothermic peak comes from the t-$MoSi_2$ formation. From this, it is concluded that h-$MoSi_2$ was the first crystalline phase of the Mo/Si multilayer thin film during solid-state reaction and was changed to t-$MoSi_2$ as the reaction temperature increased.

From the Kissinger plot [8] based on the data in Fig. 1, the activation energies of h-$MoSi_2$ and t-$MoSi_2$

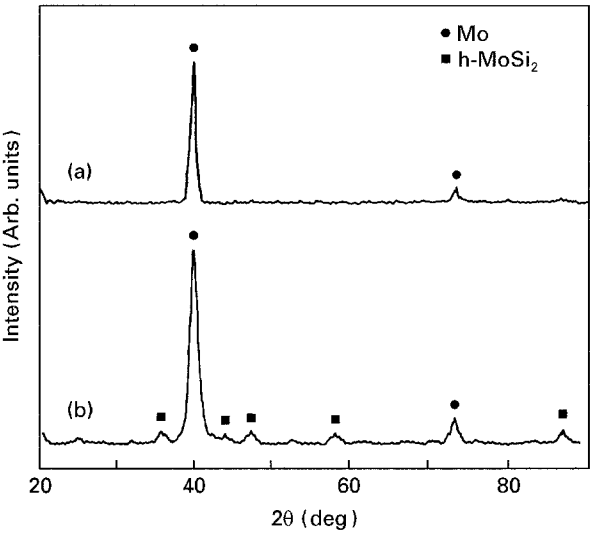

Figure 2 XRD patterns for Mo/Si thin films (a) as-deposited and (b) heated to 630 °C.

formation were obtained as 1.5 and 7.8 eV, respectively. The larger activation energy implies a higher energy barrier for phase formation. Therefore, it can be understood that t-$MoSi_2$ is more difficult to form than h-$MoSi_2$, as obtained in this experiment.

The mechanism of new-phase formation on thin films has been understood through two basic models,

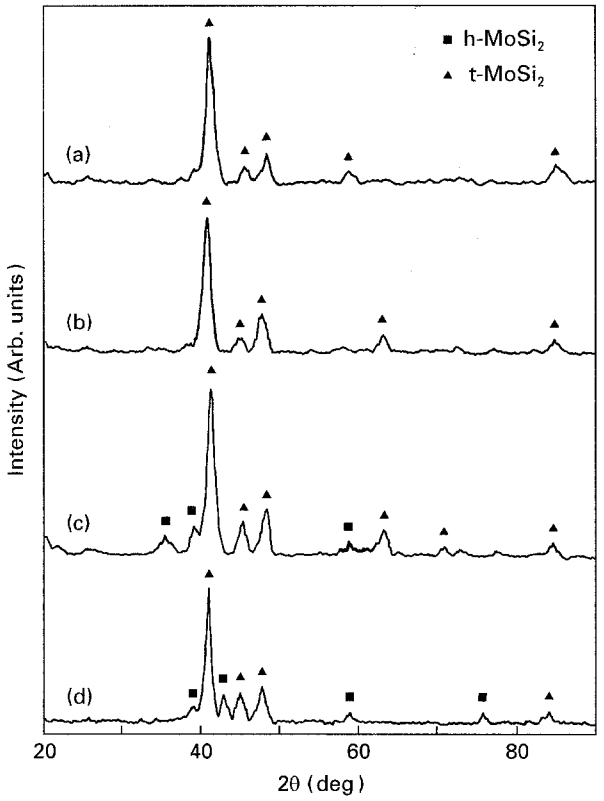

Figure 3 XRD patterns for samples heated to 700 °C at various scanning rates: (a) 20, (b) 10, (c) 5 and (d) 2.5 °C min^{-1}.

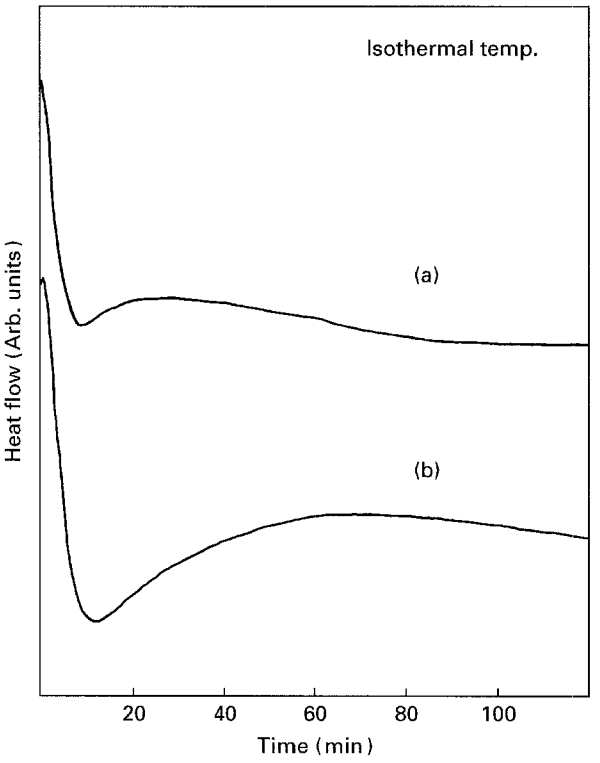

Figure 4 Isothermal DSC traces for Mo/Si multilayer thin films heated to (a) 550 °C and (b) 630 °C.

the growth-control model [9] and the nucleation model [10]. In the growth-control model, it is presumed that nucleation can very easily occur, and the fastest growing phase is formed during deposition or heat treatment. In the nucleation model, a phase with either a fastest nucleation rate or a smaller nucleation barrier is formed. While the interfacial reaction rate and interdiffusion rate act as essential variables for the growth-control model, the interfacial energy and thermodynamic driving force are considered essential for the nucleation model.

Isothermal DSC curves may appear in different forms depending on (i) one-dimensional growth without nucleation, and (ii) nucleation and further growth [11]. That is, in the case of the growth-control reaction, the amount of heat released maintains a constant value at the initial interface-controlled stage, but decreases as time passes and moves to the diffusion-controlled stage. On the other hand, in the case of nucleation reaction, the amount of heat released initially increases due to the exothermic reaction and then decreases with increasing time.

In order to identify the mechanism of h-$MoSi_2$ and t-$MoSi_2$ formation, isothermal DSC analysis was carried out for 2 h at 550 and 630 °C, and the results are shown in Fig. 4. Both reactions of h-$MoSi_2$ and t-$MoSi_2$ formation show an exothermic peak after 10 min, and after that no change of heat is detected. Therefore, it can be ascertained that the formation of h-$MoSi_2$ and t-$MoSi_2$ is the nucleation-controlled step. Loopstra *et al.* [12] also reported that the formation of h-$MoSi_2$ is the nucleation-controlled step and t-$MoSi_2$ is formed by new nucleation of h-$MoSi_2$.

3.2. Analysis of the solid-state amorphization reaction

It is well known that the formation of amorphous phase by solid-state diffusion is an exothermic reaction and its DSC trace shows a smooth and broad peak compared to a sharp peak of crystalline phase. A broad DSC peak, such as that found in the Ni/Zr system [13], where amorphous phase is easily formed, was not observed in this experiment. This result agrees with other reports that amorphous silicide did not form at the molybdenum and silicon interface. It was also confirmed by XRD analysis that the solid-state amorphization reaction did not occur in the Mo/Si multilayer thin film.

The basic condition for the occurrence of solid-phase amorphization reaction in terms of thermodynamics, is lowering of the free energy of the system through amorphous phase formation. However, an amorphous phase is metastable compared to a crystalline phase. Thus, it is inappropriate to determine the exact basis for the amorphous phase formations only in terms of thermodynamic aspects; kinetic factors should also be considered. In other words, if one element diffuses much faster than others, the atomic arrangement of the crystalline phase cannot occur and the formation of an amorphous phase with a short-range order becomes possible. Recently, Kwak *et al.* [6] have proposed the EDF (effective driving force) concept which includes all factors related to thermodynamic driving force and kinetics. With this concept as a basis for the solid-state amorphizing tendencies, this research was aimed at comparing the predicted results with the experimental results.

An EDF is determined by multiplying the maximum free-energy difference between the physical mixture of

two elements and the amorphous phase, by the effective radius ratio of the diffusing atom at the interstitial site of the matrix.

The maximum free energy difference as a thermodynamic driving force, concerning the amorphous phase formation, can be obtained from Equation 1 which shows the free-energy change following the amorphous phase formation.

$$\Delta G = X_A \Delta G_A^{a-c} + X_B \Delta G_B^{a-c} + \Delta G^M \quad (1)$$

here ΔG_A^{a-c} signifies the free-energy difference between the crystalline and amorphous phases of element A, and ΔG_B^{a-c} that of element B. ΔG^M is the mixed free-energy difference between amorphous phases. X_A and X_B are the mole fractions of elements A and B, respectively. Supposing that the amorphous phase is an undercooled liquid, the free-energy difference between the crystalline phase and the undercooled liquid can be expressed as follows, using Gong and Hentzell's method [14].

$$\begin{aligned}\Delta G^{a-c} &= \Delta H^{a-c} - T\Delta S^{a-c} \\ &= \Delta H_f(T_m - T)/T_m + (T \ln 2 - T_m/2)\Delta c_p\end{aligned} \quad (2)$$

The free-energy difference value (ΔG^M) from the mixing of amorphous phases in Equation 1 can be obtained from the ΔH^M equation based on the Miedema's theory [15] and the ΔS^M equation derived from the mixing entropy change of an ideal solution

$$\begin{aligned}\Delta G^M &= \Delta H^M - T\Delta S^M \\ &= f(X^s)gP[-e(\Delta\phi^*)^2 + Q/P(\Delta n_{ws}^{1/3})^2 \\ &\quad - R/P] + RT(X_A \ln X_A + X_B \ln X_B)\end{aligned} \quad (3)$$

where $f(X^S)$ and g are compositional functions, and X^S is the surface composition, e is the elementary charge, $\Delta\phi^*$ the chemical potential difference of electrons, and n_{ws} the electronic density. V_A and V_B are the molar volumes of elements A and B. P, Q and R are constants that vary according to the systems.

On the other hand, the radius ratio that shows the kinetic factor of amorphous phase formation, can be obtained from the effective radius of the matrix interstitial site and the atomic radius of the diffusing atom. In order to figure out the effective radius of the matrix interstitial site, it is necessary to measure the distance from the centre of the interstitial site of the matrix element to the centre of the nearest matrix atom, from which the ionic radius of the matrix atom is subtracted. The effective radius of the matrix interstitial site is calculated with respect to tetrahedral and octahedral sites, and by selecting a larger value of the two, the radius ratio is determined [16]

$$\text{effective radius ratio} = \frac{\text{effective radius of matrix interstitial site}}{\text{radius of diffusing atom}} \quad (4)$$

The EDF is expressed as the product of ΔG_{max} and radius ratio, $R_{m/d}$

$$\text{EDF} = -R_{m/d}\Delta G_{max} \quad (5)$$

In the Mo/Si system, the calculated values of maximum free-energy difference and radius ratio are 7.91 kJ mol^{-1} and 0.77, respectively. Thus, the effective driving force related to the solid-state amorphization in Mo/Si system is $-R_{m/d}\Delta G_{max} = 0.77 \times 7.91 = 6.09$ kJ mol^{-1}. Kwak *et al.* [6] suggested 15 kJ mol^{-1} as the standard EDF, and predicted that when the EDF level exceeds this value, an amorphization reaction will occur by solid-state diffusion. Therefore, the amorphization reaction is not expected to occur in the Mo/Si system, which is in accordance with this experimental results.

3.3. Examination of phase sequence

h-$MoSi_2$ was formed as the first crystalline phase and t-$MoSi_2$ as the second by solid-state reaction in the Mo/Si multilayer thin film. The first crystalline phases reported to date are Mo_3Si, Mo_5Si_3, h-$MoSi_2$ and t-$MoSi_2$. But recent experiments show two forms of silicides, h-$MoSi_2$ and t-$MoSi_2$. Mo_3Si is formed by an oxide layer existing between the molybdenum layer and the silicon substrate [17], and Mo_5Si_3 is known to form when the molybdenum layer is excessively contaminated by oxygen [18]. Because NaCl was used as the substrate in this experiment, and molybdenum and silicon were deposited without breaking the vacuum, it can be assumed that the oxide layer was not formed. It was confirmed that the amount of contaminated oxygen was below 1 at % throughout the thin-film layer by AES analysis which was not shown.

On the other hand, according to the equilibrium phase diagram of the Mo/Si system [19] shown in Fig. 5, Mo_3Si, Mo_5Si_3, and t-$MoSi_2$ (α-$MoSi_2$) can only exist. Among these, t-$MoSi_2$ is considered to be the most stable phase because it has the largest negative value of bulk free energy. And it is predicted to be the first phase by Walser and Bene [20] and Pretorius [7].

The first crystalline phase can be predicted by a diagram of effective heat of formation shown with the equilibrium phase diagram in Fig. 5. $Mo_{0.02}Si_{0.98}$, having the lowest eutectic temperature of 1400 °C, is the effective concentration in the equilibrium phase diagram in the Mo/Si system. Mo_3Si, Mo_5Si_3 and t-$MoSi_2$ are the possible compounds that can be formed. Of these, t-$MoSi_2$ is predicted to form as the first phase because it has the largest negative value of effective heat of formation at the effective concentration.

However, other recent studies confirmed h-$MoSi_2$ as the first phase. Here, by comparing the interface free energy and crystal structure of h-$MoSi_2$ and t-$MoSi_2$, these results can be explained. When a new phase is formed, the bulk free energy is decreased, but the interface free energy is increased because a new interface is created. Thus, nucleation is the result of competition between the negative bulk free energy and the positive interface free energy. When comparing only

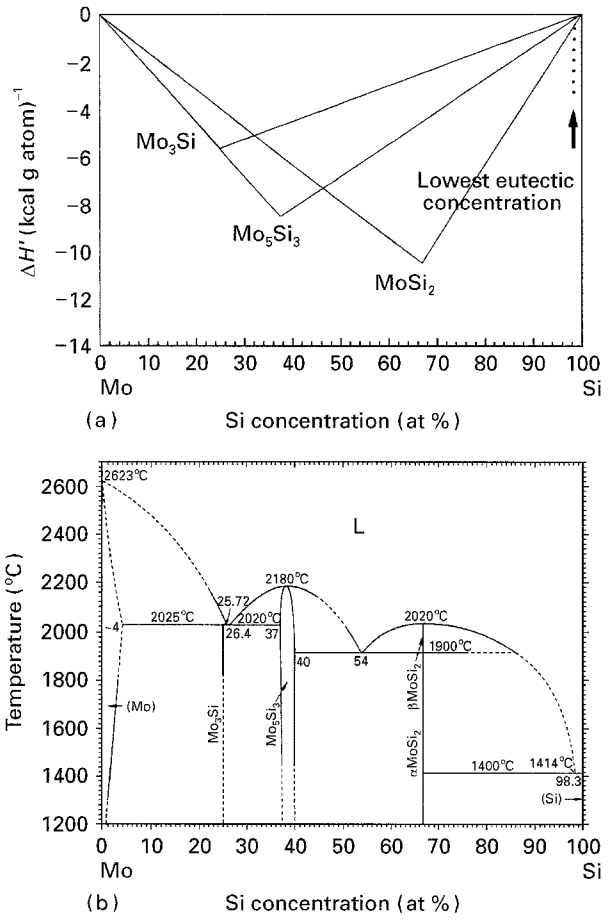

Figure 5 (a) Effective heat of formation diagram and (b) phase diagram for the Mo/Si binary system.

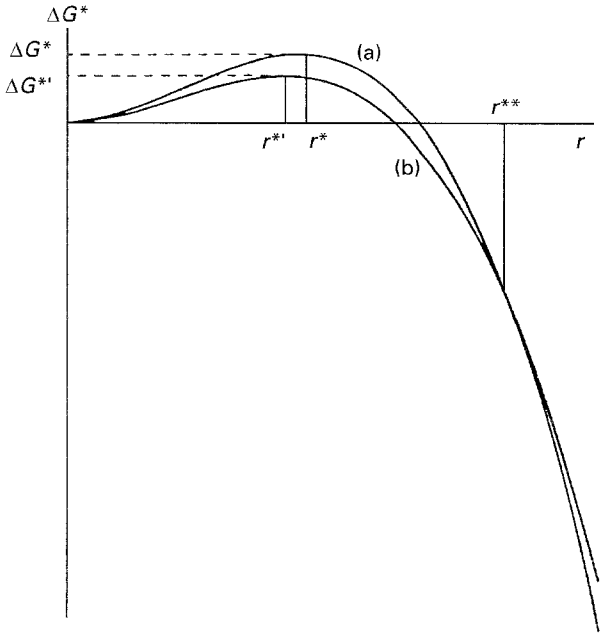

Figure 6 Proposed free energy of cluster formation [21]: (a) *t*-$MoSi_2$ and (b) *h*-$MoSi_2$. ΔG^*, r^* are the nucleation barrier and critical cluster size for nucleation of *t*-$MoSi_2$; $\Delta G^{*\prime}, r^{*\prime}$ are the nucleation barrier and critical cluster size for nucleation of *h*-$MoSi_2$; r^{**} is the critical cluster size for transformation of *h*-$MoSi_2$ to *t*-$MoSi_2$.

the bulk free energy, t-$MoSi_2$ is more stable than h-$MoSi_2$. But, if the interface free energy of h-$MoSi_2$ is lower than that of t-$MoSi_2$, the free energy change for cluster formation can be displayed as in Fig. 6 [21].

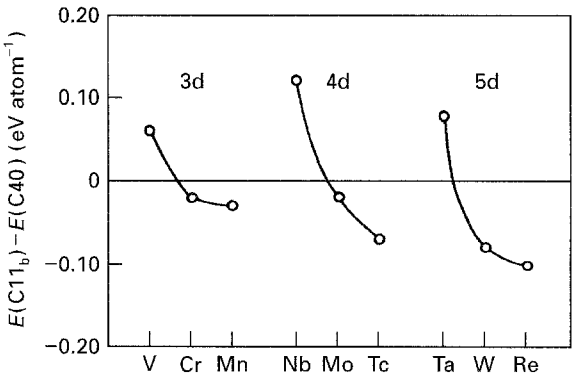

Figure 7 Calculated total energy differences between $C11_b$ and C40 structure for MSi_2 compounds [23].

From this, it can be determined that if the interface free energy is small, the energy barrier and critical radius of the cluster also become small. Therefore, the nucleation of h-$MoSi_2$ is easier than that of t-$MoSi_2$. This explanation is applicable to the results of this study; the formation of both h-$MoSi_2$ and t-$MoSi_2$ is nucleation controlled, and the activation energy of each is 1.5 and 7.8 eV, respectively. Owing to the greater energy barrier of t-$MoSi_2$, h-$MoSi_2$ is formed as the first crystalline phase and t-$MoSi_2$ as the final phase.

If the radius of the cluster increases beyond r^{**}, the free energy of t-$MoSi_2$ will become smaller than that of h-$MoSi_2$, and phase transformation from h-$MoSi_2$ to t-$MoSi_2$ will be predicted. Here, the formation of t-$MoSi_2$ is possible by surmounting the high nucleation barrier as the temperature increases. The fact that in Fig. 1 the DSC peak of h-$MoSi_2$ becomes smaller as that of t-$MoSi_2$ becomes larger with increasing heating rate, can be explained in this perspective. That is, because a high temperature is acquired more rapidly by increasing the heating rate, the formation of h-$MoSi_2$ is decreased and that of t-$MoSi_2$, having a high nucleation barrier, has become easy.

On the other hand, the crystal structures of t-$MoSi_2$ and h-$MoSi_2$ were compared. The crystal structures of the transition metal disilicide are usually tetragonal $C11_b$, hexagonal C40, and orthorhombic C54 [22]. The structures of t-$MoSi_2$ and h-$MoSi_2$ are $C11_b$ and C40, respectively. These have different structural energies because they have different stacking structures [23]. The differences in structural energy calculated for the elements of groups V, VI, and VII are shown in Fig. 7. In the case of $MoSi_2$, the value is approximately 0.025 eV atom^{-1}

$$E(\mathrm{C40}) - E(\mathrm{C11_b}) \fallingdotseq 0.025\ \mathrm{eV\,atom^{-1}} \quad (6)$$

Considering this value, hexagonal C40 is a metastable phase having a higher energy compared to tetragonal $C11_b$. Therefore, it can be thought that h-$MoSi_2$, which was formed first, continues to decrease the energy of the system, by forming more stable t-$MoSi_2$.

4. Conclusion

The solid-state reaction of Mo/Si multilayer thin films deposited by the r.f. magnetron sputtering method was

examined using DSC and XRD. In constant scanning-rate DSC from 30–700 °C, two exothermic peaks were observed, and these were attributed to the formation of h-$MoSi_2$ and t-$MoSi_2$. The activation energies of h-$MoSi_2$ and t-$MoSi_2$ formation were 1.5 and 7.8 eV, respectively. Through isothermal DSC analysis, the nucleation was found to be the rate-controlling mechanism for each of the silicide formation DSC analyses. No amorphous phase was formed in the Mo/Si system, which agrees with the prediction by the concept of the effective driving force. The first crystalline phase was observed to be h-$MoSi_2$ and as the temperature increased, h-$MoSi_2$ was transformed into t-$MoSi_2$. h-$MoSi_2$ was considered to have a lower interface free energy than t-$MoSi_2$.

References

1. M. A. NICOLET and S. S. LAU, "VLSI Electronics Microstructure Science", Vol. 6 (Academic Press, New York, 1983).
2. U. GÖSELE and K. N. TU, *J. Appl. Phys.* **66** (1989) 2619.
3. K. N. TU, G. OTTAVIANI, U. GÖSELE and H. FÖIL, *ibid.* **54** (1983) 758.
4. F. BORDEAUX and A. R. YAVARI, *ibid.* **67** (1990) 2385.
5. A. PETFORSD-LONG, M. B. STEARNS, C.-H. CHANG, S. R. NUTT, D. G. STEARNS, N. M. CEGLIO and A. M. HAWRYLUK, *ibid.* **61** (1987) 1422.
6. J. S. KWAK, E. J. CHI, J. D. CHOI, S. W. PARK, H. K. BAIK, M. G. SO and S. M. LEE, *J. Korean Vac. Soc.* **2** (1993) 50.
7. R. PRETORIUS, A. M. VREDENBERG and F. W. SARIS, *J. Appl. Phys.* **70** (1991) 3636.
8. H. E. KISSINGER, *Anal. Chem.* **29** (1957) 1702.
9. U. GÖSELE and K. N. TU, *J. Appl. Phys.* **53** (1982) 3252.
10. F. M. d'HEURLE, *J. Mater. Res.* **3** (1988) 167.
11. L. A. CLEVENGER and C. V. THOMPSON, *J. Appl. Phys.* **67** (1990) 1325.
12. O. B. LOOPSTRA, W. G. SLOOF, T. H. DE KEIJSER, E. J. MITTEMEIJER, S. RADELAAR, A. E. KUIPER and R. A. M. WOLTERS, *ibid.* **63** (1988) 4960.
13. E. J. COTTS and W. L. JOHNSON, *Phys. Rev. B.* **37** (1988) 9049.
14. S. F. GONG and H. T. G. HENTZELL, *J. Appl. Phys.* **68** (1990) 4542.
15. A. R. MIEDEMA, *Philips Tech. Rev.* **36** (1976) 217.
16. F. Y. SHIAU, PhD thesis, University of Wisconsin-Madison (1990).
17. C.-D. LIEN and M. A. NICOLET, *J. Vac. Sci. Technol. B* **2** (1984) 738.
18. F. NAVA, G. MAJNI, P. CANTONI, G. PIGNATEL, G. FERLA, P. CAPPELLETTI and F. MORI, *Thin Solid Films* **94** (1982) 59.
19. T. B. MASSALSKI, "Binary Alloy Phase Diagrams" (American Society for Metals, Metals Park, Ohio, 1986).
20. R. M. WALSER and R. W. BENE, *Appl. Phys. Lett.* **28** (1976) 624.
21. C. M. DONALD and R. J. NEMANICH, *J. Mater. Res.* **5** (1990) 2854.
22. W. D. PEARSON, "The Crystal Chemistry and Physics of Metals and Alloys" (Wiley, New York, 1972).
23. J.-H. XU and A. J. FREEMAN, *Phys. Rev. B* **40** (1989) 11927.

Received 19 September 1994
and accepted 1 December 1995